Journal of Crystal Growth 350 (2012) 33–37

Contents lists available at SciVerse ScienceDirect

Journal of Crystal Growth

journal homepage: www.elsevier.com/locate/jcrysgro

Structural and optical properties of thick freestanding AlN films prepared by hydride vapor phase epitaxy

J.A. Freitas Jr.[a,*], J.C. Culbertson[a], M.A. Mastro[a], Y. Kumagai[b], A. Koukitu[b]

[a] Naval Research Laboratory, Washington DC 20375, USA
[b] Department of Applied Chemistry, Tokyo University of Agriculture and Technology, Koganei, Tokyo 184-8588, Japan

ARTICLE INFO

Available online 30 December 2011

Keywords:
A1. Luminescence
A1. Raman
A1. Impurity
A2. Freestanding
A3. Grown from vapor
B1. Nitrides

ABSTRACT

The morphology, structural and optical properties of void-assisted freestanding HVPE-AlN films were investigated by a combination of non-destructive microscopic and spectroscopic techniques. The freestanding approximately 80 μm thick clear film has a wurtzite crystalline structure with remarkable properties around the central film region. The E_2(high)-phonon frequency coincides with reported stress-free film phonon frequency. The low temperature luminescence study of the growth and interface sides of the film is consistent with the incorporation of a high concentration of oxygen impurities. These results are promising as the growth method amenable to the production of freestanding stress-free large area substrates for epitaxial growth.

Published by Elsevier B.V.

1. Introduction

In spite of the potential electronic device applications, optoelectronic devices are the driving force of AlN based material research. Deep ultraviolet laser diodes and light emitting diodes with sub-300 nm peak emission are important for a number of biological, chemical, and technological applications. The lack of a large-area and low-cost native substrate has compelled device research to employ sapphire substrates for AlN and AlGaN film deposition. To prevent cracking, films must be grown thin and the doping level must be limited [1], which results in highly defective and stressed heteroepitaxial films. As a result, the film electrical and thermal properties limit the wall-plug device efficiency to typically 1–2%. Clearly, the use of a native substrate will be crucial to achieving high yield for high performance devices.

Despite recent progress on the growth of high crystalline quality bulk AlN crystals by physical vapor transport (PVT) and sublimation-and-recondensation (S&R), the size and commercial availability of this material is still limited [2]. Therefore, investigations into growth or deposition processes that result in large area freestanding substrates are of great interest. Hydride vapor phase epitaxy (HVPE) has been successfully employed to deposit AlN, AlGaN, and multi layer structures on a variety of 2 to 3 in. foreign substrates [3,4]. AlN films deposited on Si and SiC substrates, removed from the substrates by etching techniques, were used as seeds to grow AlN boules with a diameter ranging from 0.5 to 1.75 in. Selected wafers were employed as substrates to deposit epitaxial AlN films with improved structural and optical properties [5]. A considerable improvement in the AlN freestanding substrate quality, yield and manufacturing cost could be achieved if a self-separation method is developed. Self-separation of HVPE grown GaN films of 2 and 3 in. in diameter was successfully accomplished by a void-assisted separation method [6]. Due to the higher AlN growth temperature [7] and chemical reactivity one may expect additional challenges in developing a self-separation method for HVPE-AlN films.

Recently, it was reported that interfacial voids formed between (0001) sapphire substrate and thick AlN films resulted in the preparation of freestanding AlN thick films [8]. Heat treatment of 100–200 nm thick AlN films, grown at 1065 °C, performed under gas flow mixture of H_2, N_2, and NH_3 at 1450 °C, generates a large density of voids beneath the thin AlN film. The self-separation of the subsequently grown thick AlN film occurs during the post-growth cooling. The growth surface of the film is specular. The back surface is mirror smooth in the center but does display a roughened surface at the periphery of the sample.

A combination of non-destructive microscopic and spectroscopic techniques was employed to probe the morphology, an structural and optical properties of void-assisted freestanding HVPE-AlN films. The results confirm that the 8 mm × 6 mm area size and ~80 μm thick freestanding film has a wurtzite crystalline structure and suggests that a scaled growth process could provide large area substrates for epitaxial growth.

2. Growth and experimental details

AlN films with improved properties have been previously deposited at temperatures above 1200 °C on (0001) sapphire substrates [7].

* Corresponding author. Tel.: +01 202 404 4536; fax: +01 202 767 1165.
E-mail address: jaime.freitas@nrl.navy.mil (J.A. Freitas Jr.).

0022-0248/$ - see front matter Published by Elsevier B.V.
doi:10.1016/j.jcrysgro.2011.12.018

The increasing difference between AlN and sapphire thermal expansion coefficients with increasing temperature, results in severe cracking of the AlN heteroepitaxial film and sapphire substrate during the post-growth cooling to room temperature. It was observed that AlN and sapphire decompose by reaction with the H_2 carrier gas at temperatures above 1200 °C, and the AlN decomposition could be suppressed with the addition of NH_3 to the carrier gas containing H_2 [8]. Furthermore, it was verified that a 1450 °C thermal treatment of a 100 nm thick AlN film deposited at 1065 °C, carried out in a mixed gas flow of H_2, N_2, and NH_3, led to a partial decomposition of the sapphire surface and the formation of voids underneath the thin AlN film. In addition, thick AlN films subsequently deposited at 1450 °C on the heat treated thin AlN layer self-released from the sapphire substrate during the post-growth cool down to room temperature [8]. This approach was employed to produce the free-standing AlN films evaluated in this work.

The studied free standing AlN film was deposited in a multi-zone horizontal hot-wall atmospheric pressure reactor. The resistive heating susceptor is able to reach temperatures up to 1500 °C. $AlCl_3$ was generated in the upstream region of the reactor by flowing HCl gas over Al metal at 500 °C [9]. The $AlCl_3$ and NH_3 gasses were introduced separately into the downstream region maintained at 540 °C. The chemically cleaned (0001) sapphire substrate was placed on the susceptor and the temperature was raised to 1065 °C to deposit the low temperature 200 nm thick AlN layer, or the intermediate layer. The temperature of the sample was raised to 1450 °C in a H_2/N_2 mixed carrier gas flow with additional NH_3 for a specific time to form the voids beneath the intermediate AlN layer. The thick AlN film was grown at 1450 °C for 4 h. After the completion of the thick AlN deposition, the sample was cooled down to room temperature under NH_3 atmosphere to avoid surface AlN decomposition. Detailed discussions of the film growth conditions, void formation, and self-separation mechanism is presented elsewhere [10].

The growth front surface of the ~80 μm thick freestanding AlN film is specular but an SEM micrograph (Fig. 1a) shows the presence of surface features such as indentations (≤ 30 μm) and a "fish scale" of a few hundred micrometers in size. The interface (back surface) of the film, shown in Fig. 1b, appears smooth and transparent at the center, but has a number of large pits (10–50 μm). The region around the clear central region is rough and has large density of smaller diameter pits that increases in concentration near the periphery of the film. Also observed on this face are few straight lines, located between the center of the sample and the small pit region, which under larger magnification shown that the presence of small dots, similar to dislocation lines decorating grain boundaries. Micro-cracks are easily observed by conventional bright or dark field optical microscopy. We have not observed features similar to that reported by other, which have been identified as micro-cracks in AlN films deposited on sapphire substrates [11].

X-ray diffraction (XRD) and Raman scattering (RS) spectroscopies were used to investigate the structural properties of the thick freestanding AlN film. Panalytical X'Pert XRD system with a Cu Kα source has a typical sampling depth at an incident angle of about 2 μm.

The Raman spectra were acquired with a home assembled micro-Raman spectrometer, which is comprised of a 0.5 m single spectrometer fitted with an 1800 groves/mm grating, and a liquid nitrogen cooled back-thinned/deep-depleted CCD sensitive in the visible-near IR spectral range, and a 532 nm solid state laser. The typical laser spot size was 1 μm, and the laser intensity was of about 5 mW. Polarizers were used to control the laser and select the scattered light polarization.

The cathodoluminescence (CL) measurements were carried out with a commercial electron gun installed in an ultra high vacuum chamber. Electron beam (e-beam) currents between 1 and 2 μA and e-beam energies between 7 and 12 keV were commonly used. The spot size was set about 2 mm to achieve low excitation density. The light emitted by the samples was collected and focused by a set of lens, and flat and parabolic mirrors with matching numerical apertures, and dispersed by a double spectrometer fit with 1200 grooves/mm gratings. The dispersed light was detected by an UV-sensitive GaAs photomultiplier tube connected to a computer-controlled photon counter. The samples were mounted on a cold finger cryostat with a controlled temperature varying from 5 to 330 K.

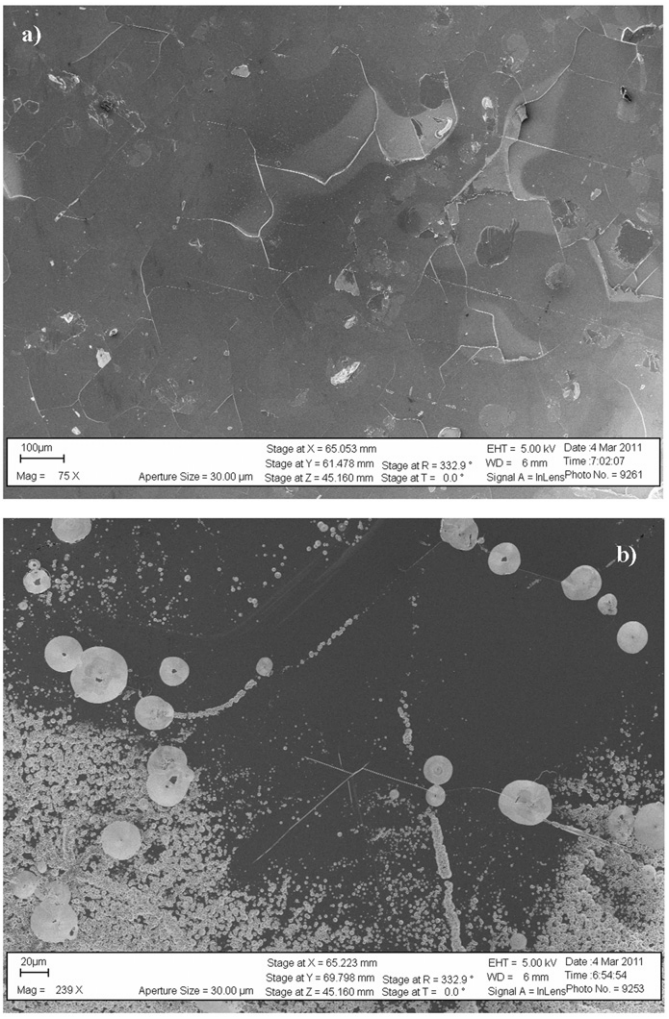

Fig. 1. Surface SEM micrograph of the (a) growth surface and (b) interface surface of the ~80 μm thick freestanding AlN film. Pits are observed only on back surface of the film.

3. Experimental results and discussion

The measured diffracted peaks are a summation of the diffraction broadening from grains and defects within the approximate 1 mm^2 sample area. The FWHM of the XRD rocking curve was 1.4° for the symmetric (0004) reflection (Fig. 2). The diffraction broadening convolutes the peaks over sampled area, and XRD does not preclude high quality grains within a matrix of moderate defectivity.

The wurtzite crystal structure of AlN belongs to the C_{6v}^4 space group, which according to group theory predicts the contribution of the Brillouin zone-center optical modes $A_1+2B_1+2E_2$ [12]. With exception of the silent B_1 modes, all the other modes are

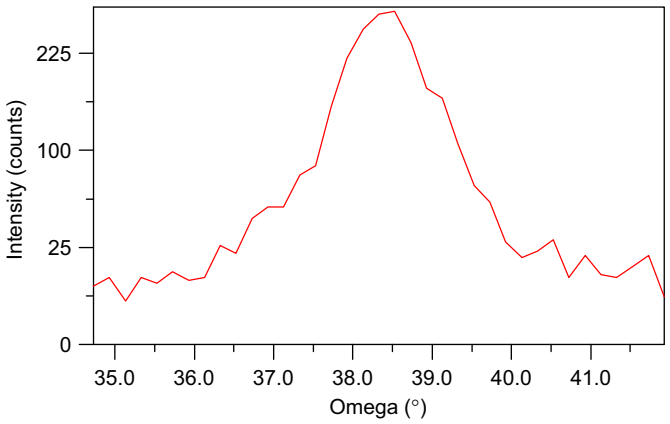

Fig. 2. XRD ω-scan of the AlN (0004) peaked displayed a FWHM of 1.4°.

allowed in Raman scattering and have been observed [13]. The A_1 and E_1 optical phonon modes split into longitudinal optical (LO) and transversal optical (TO) due to polar nature of AlN. The identifications of all these phonons modes have been achieved by comparing polarized Raman scattering studies with the theoretical predictions obtained through the Raman tensors.

The room temperature Raman scattering study of a freestanding AlN film was carried out under back scattering geometry using the home setup micro-Raman spectrometer described above. In addition to the E_2^1 (E_2 low), E_2^2 (E_2 high), and A_1(LO) allowed phonons for $z(y,y)\bar{z}$ scattering geometry, we also observed weak not-allowed A_1(TO) and E_1(TO) phonons, and a not yet identified peak at $\sim$282 cm^{-1} (Figs. 3a–d). For $z(x,y)\bar{z}$ scattering geometry only the E_2 phonons should be observed, but we also observed weak A_1(TO) and E_1(TO) phonons. The breaking of the scattering selection rules can result from sample misorientation, polarization leakage, and internal laser back-reflection.

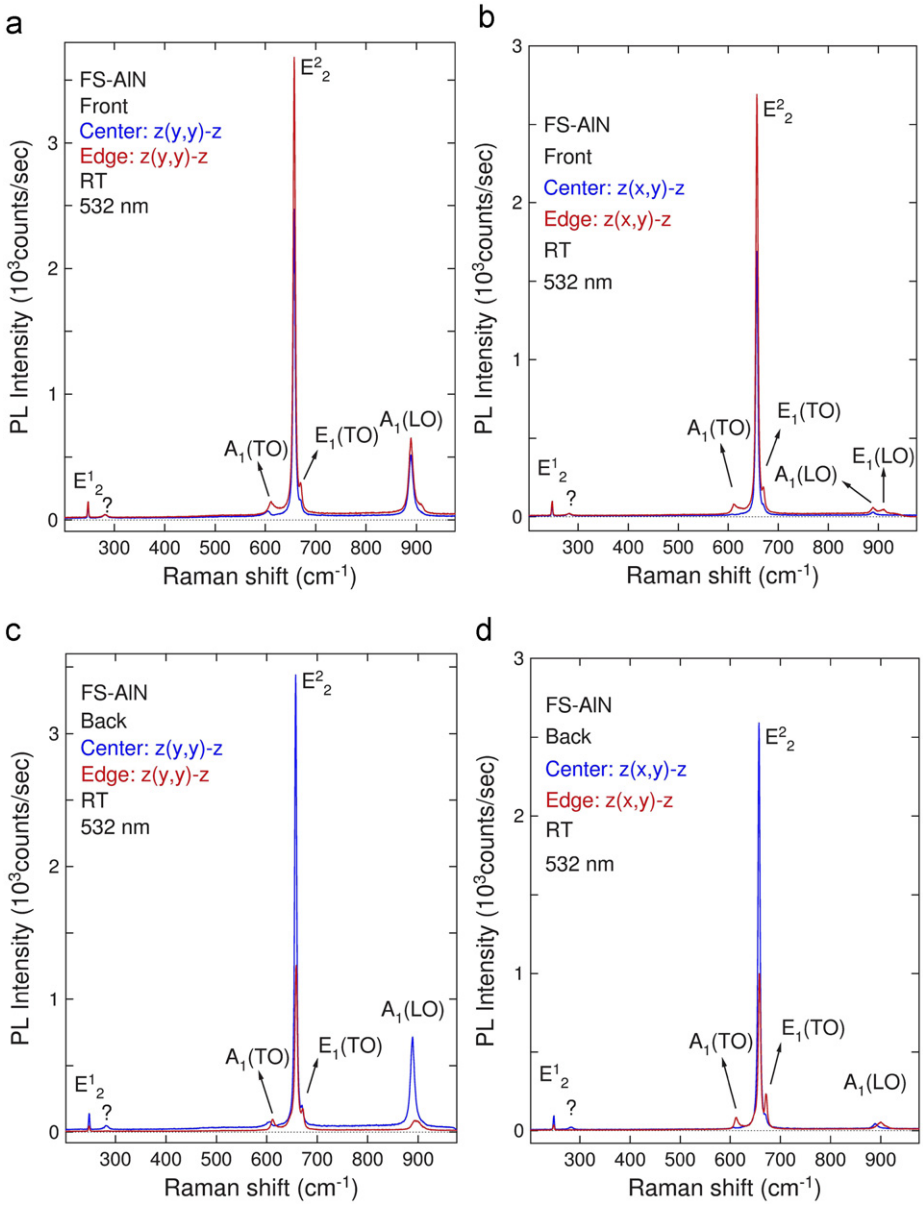

Fig. 3. Polarized Raman spectra of the freestanding AlN film measured at the: film growth surface (Front) (a) $z(y,y)\bar{z}$ and (b) $z(x,y)\bar{z}$ scattering geometry; and interface side of the film (Back) (c) $z(y,y)\bar{z}$ and (d) $z(x,y)\bar{z}$ scattering geometry. Note the presence of non-allowed phonon in the spectra measured at the sample boundary.

Raman spectra acquired near the edge of the sample show a contribution from the E_1(LO), which is allowed only for $x(y,y)\bar{x}$ and $x(z,z)\bar{x}$ scattering geometry. This indicated the existence of a considerable degree of film grain misorientation at this film region, introduced by film edge bowing or the large concentration of defects. Note that there is a large concentration of pits in the region near the edge of the sample, as indicated in Fig. 1b., which could be responsible for the observation of non-allowed vibrational modes. The frequencies of the E_2^1 (E_2 low), E_2^2 (E_2 high), and A_1(LO) phonons are 247.8 cm^{-1}, 657.5 cm^{-1}, and 888.9 cm^{-1}, respectively. The estimated spectral resolution is 0.7 cm^{-1}. The 657.5 cm^{-1} frequency value of the E_2^2 phonon, which is conveniently used for film stress measurements, acquired near the center of the film (at the front and back surface, represented in Figs. 3a and b) is very close to the value of 657.4 cm^{-1} determined for zero-stress film [14,15]. Therefore, within the experimental error of the published results and of our measurements, it could be stated that the central part of the film is stress free. Note that the same E_2^2 phonon frequency value was also obtained at the front face, near the edge of the sample. However, measurements performed at the back face and near the sample edge yield E_2^2 frequency of 658.6 cm^{-1}, which correspond to a residual compressive stress of 0.27 GPa (Figs. 3c and d). The values of the E_2 and A_1(LO) phonon frequencies and FWHM of the FS AlN films are larger than the values reported by Tischler and Freitas for high crystalline quality self-nucleated bulk AlN, indicating that the films crystalline quality (high defect concentration) and high impurity concentration plays an important role on the material properties [16,17]. The observed line shape asymmetry of the LO phonons, especially in measurements carried out near the sample periphery, may result from a high concentration of impurities, which perturbs the intrinsic crystal vibrational mode [18]. Also, the larger concentration of gross defects could change the local crystal orientation allowing the observation of symmetry-prohibited phonons or mixed phonon modes [19], which will overlap with the allowed phonon modes. A third possibility, but less likely because it is difficult to achieve high doping level in AlN, is the presence of high concentration of free-carriers, which strongly couple with the A_1(LO) phonon [20]. A more detailed RS scattering study must be carried to find out the mechanisms responsible for these anisotropies, which will require selected samples and it is out of the scope of the present work.

Fig. 4. shows the low-temperature CL spectra measured at the front and back surfaces of the freestanding AlN films. Both spectra are similar, despite of the difference in the relative intensity of the deep emission band observed at ~3.3 eV, represented as VB (violet band) in Fig. 4. Previous low temperature CL measurements performed on S&R bulk AlN and HVPE substrates, and epitaxial AlN films showed the presence of two additional bands at ~4.5 eV (UVB) and ~6.0 eV (NBE). The 4.5 eV band has not been identified yet. The 6.0 eV band has been associated with recombination processes involving the annihilation of free excitons and excitons bound to relatively shallow donor and acceptor impurities [21,22]. Similar CL spectra have also been observed in samples grown by thermo-decomposition of aluminum chloride monoammoniate [23]. The observation of similar luminescence spectra from samples grown by different methods clearly indicates the pervasive character of the defects associated with these emission bands. It is quite interesting that only the ~3.3 eV band is observed in the CL spectra of the freestanding/self-separated HVPE films, under the present experimental conditions. It was previously reported that the NBE emission in AlN decreases with increasing incorporation of oxygen [24]. Although not mentioned, the intensity of the emission band at ~4.5 eV also reduces with increasing oxygen concentration, and the ~3.3 eV emission band, assigned to V_{Al}–O complex, is the dominant spectral feature

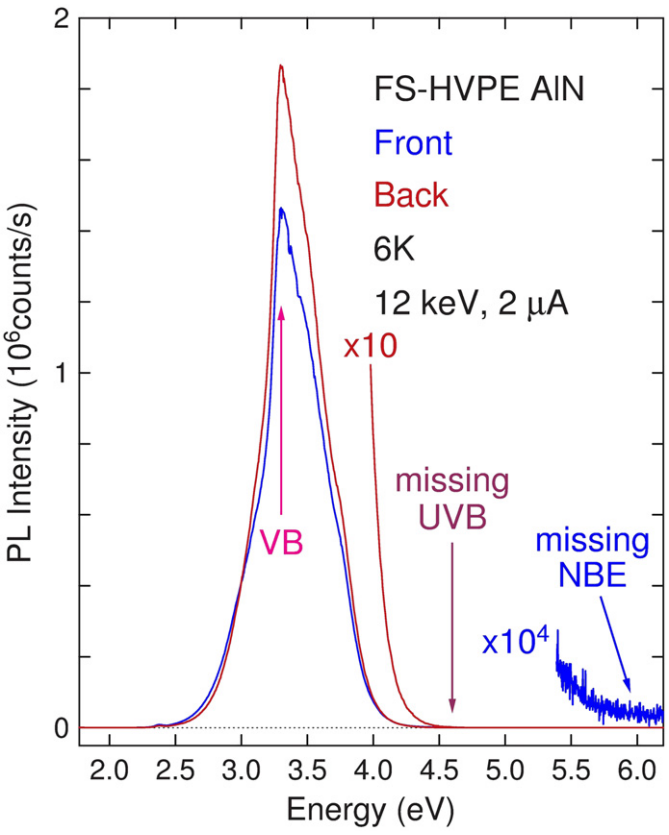

Fig. 4. Low temperature cathodoluminescence spectra acquired at the growth and interface surfaces of the self-released AlN film. The ~3.3 eV emission band dominates the visible–UV probed spectral range. Note that the 4.5 eV and the 6.0 eV bands are not observed in these spectra at this excitation condition.

observed in the luminescence spectra of samples with oxygen concentration around 10^{20} cm^3 [24]. Note that the ~3.3 eV emission band peak intensity acquired at the back of the film is larger than that acquired at the front surface (Fig. 4), suggesting that larger incorporation of oxygen is achieved at the interface of the film with the intermediate layer and the sapphire substrate. Larger incorporation of oxygen has been observed on the interface of GaN deposited on sapphire substrates, and more recently in heteroepitaxial AlN films [25]. A detailed SIMS impurity trace analysis is planned to measure the concentration of oxygen incorporated in films grown by the present growth method. For room temperature absorption measurements on similar samples the transmittance varied from 65% to 55% between 1 μm and 300 nm, and decreased rapidly from 280 nm to 208 nm [10].

4. Summary

The morphology and the structural and optical properties of a thick and crack-free freestanding AlN films grown by void-assisted HVPE on sapphire substrate are presented. Despite the high concentration of pits on the AlN sapphire-substrate interface, the growth surface of the film is mirror smooth and is transparent at the center. The XRD and Raman scattering studies verified the wurtzite crystalline structure of the film. The coincidence of the these films E_2(high) first order allowed phonon frequency with that of stress-free E_2(high)-phonon heteroepitaxial films indicates that freestanding stress-free films can be produced. The estimated concentration of extended structural defects is typical for films deposited on non-native substrates, but an improved intermediate layer may assist on the reduction of these defects concentration.

Low temperature luminescence studies carried out at both film surfaces are consistent with high incorporation of oxygen impurities.

References

[1] V. Adivaram, A. Heidari, B. Zhang, Q. Fareed, S. Hwang, M. Islam, Asif Khan, Applied Physics Express 2 (2009) 102101.
[2] J.A. Freitas Jr., Journal of Physics D: Applied Physics 43 (2010) 073001.
[3] Yu. Melnik, D. Tsvetkov, A. Pechnikov, I. Nikitina, N. Kuznetsov, V. Dmitriev, Physics Status Solidi (a) 188 (2001) 463.
[4] D. Tsvetkov, Yu. Melnik, A. Davidov, A. Shapiro, O. Kovalenkov, J.B. Lam, J.J. Song, V. Dmitriev, Physics Status Solidi (a) 188 (2001) 429.
[5] Yu. Melnik, V. Soukhoveev, V. Ivantsov, A. Pechnikov, K. Tsvetkov, O. Kovalenkov, V. Dmitriev, A. Nikolaev, N. Kuznetsov, E. Silveira, J.A. Freitas Jr., Physics Status Solidi (a) 200 (2003) 22.
[6] T. Yoshida, Y. Oshima, T. Eri, K. Ikeda, S. Yamamoto, K. Watanabe, M. Shibata, T. Mishima, Journal of Crystal Growth 310 (2008) 5.
[7] T. Nagashima, M. Harada, H. Yanagi, Y. Kumagai, Y. Kumagai, A. Koukitu, K. Takada, Journal of Crystal Growth 300 (2007) 42.
[8] Y. Kumagai, J. Tajima, M. Ishizuki, T. Nagashima, H. Murakami, K. Takada, A. Koukitu, Applied Physics Express 1 (2008) 045003.
[9] Y. Kumagai, T. Yamane, T. Miyaji, H. Murakami, Y. Kangawa, A. Koukitu, Physics Status Solidi (c) 0 (2003) 2498.
[10] Y. Kumagai, Y. Enatsu, M. Ishizuki, Y. Kubota, J. Tajima, T. Nagashima, H. Murakami, K. Takada, A. Koukitu, Journal of Crystal Growth 312 (2010) 2530.
[11] L.H. Robins, D.K. Wickenden, APL 71 (1997) 3841.
[12] L. Bergman, M. Dutta, R.J. Nemanichi, Raman Scattering Spectroscopy and Analyses of III–V Nitride Based Materials, Raman Scattering in Material Science, Springer, Berlin, 2000. Chapter 7.
[13] J.G. Tischler, J.A. Freitas Jr., Applied Physics Letters 85 (2004) 1943.
[14] S. Yang, R. Miyagawa, H. Miyake, H. Hiramatsu, H. Harima, Applied Physics Express 4 (2011).
[15] T. Prokofyeva, M. Seon, J. Vanbuskirk, M. Holtz, S.A. Nikishin, N.N. Faleev, H. Temkin, S. Zollner, Physical Review B 63 (2001) 125313.
[16] J. Menéndez, M. Cardona, Physical Review B 29 (1982) 2051.
[17] D. von der Linde, J. Kuhl, H. Klingenberg, Physical Review Letters 44 (1968) 1505.
[18] M. Melendez, J. Menéndez, K.M. Kramer, M.O. Thompson, N. Cave, R. Liu, J.W. Christiansen, N.D. Theodore, J.J. Candelaria, Journal of Applied Physics 82 (1997) 4246.
[19] C.A. Arguello, D.L. Rousseau, S.P.S. Porto, Physical Review B 181 (1969) 1351.
[20] P. Perlin, J. Camassel, W. Knap, T. Taliercio, J.C. Chervin, T. Suski, I. Grzegory, S. Porowski, Applied Physics Letters 67 (1995) 2524.
[21] J.A. Freitas, Journal of Crystal Growth 281 (2005) 168.
[22] E. Silveira, J.A. Freitas Jr., O. Glembocki, G.A. Slack, L.J. Schowalter, Physical Review B 71 (2005) 041201. R.
[23] J.A. Freitas Jr., G.C.B. Braga, E. Silveira, J.G. Tischler, M. Fatemi, Applied Physics Letters 83 (2003) 2584.
[24] G.A. Slack, L.J. Schowalter, D. Morelli, J.A. Freitas Jr., Journal of Crystal Growth 246 (2002) 287.
[25] V. Lughi, D.R. Clarke, Applied Physics Letters 89 (2006) 241911.